A Low-Complexity Time-Domain Linear Symbol Combining Technique for PAPR Reduction in OFDM Systems

Emad Alsusa, *Senior Member, IEEE*, and Lin Yang, *Student Member, IEEE*

***Abstract*—High peak-to-average-power ratio (PAPR) is a particular disadvantage of orthogonal frequency-division multiplexing (OFDM) systems and can significantly degrade the power efficiency at the transmitter. The aim of this paper is to propose a post-inverse fast Fourier transform (IFFT) PAPR reduction method based on intelligent linear symbol combining with the objective to minimize the PAPR at the transmitter. Unlike the methods so far reported in the literature, the proposed method has a relatively low complexity and does not require external randomization sequences. This paper will also investigate the impact of the proposed method on the system's bit error rate (BER) performance and provide a closed-form analytical expression that takes into account the BER dependency on the side information bits and multiblock combination. It will be shown that the proposed technique can provide significant PAPR reductions at manageable levels of signal processing requirements while the BER degradation is relatively small.**

***Index Terms*—Orthogonal frequency-division multiplexing (OFDM), peak-to-average-power ratio (PAPR) reduction, time-domain processing.**

I. Introduction

ORTHOGONAL frequency-division multiplexing (OFDM) is expected to be the transmission scheme of choice for a number of future wireless networks after it was successfully adopted for several current high-speed wireless data transmission systems [1]–[3]. However, such a transmission technique has a major drawback related to its high peak-to-average-power ratio (PAPR) that is caused by the large envelope fluctuations of the time-domain signal. High PAPR values can lead to serious problems such as severe power penalty at the transmitter, which is not affordable in portable wireless systems where terminals are powered by battery [4], [5].

Several PAPR reduction techniques have been proposed in the literature including amplitude clipping (AC), sequence coding (SC), tone reservation (TR), and multiple signal representation (MSR) techniques such as the selected mapping (SLM) and partial transmit sequence (PTS) techniques [6]. The simplest of these is the AC technique, but it is found to cause both in-band and out-of-band distortion. On the other hand, while the SC technique could offer excellent performance on PAPR reduction, the cost in complexity and data rate loss make it unpopular. The TR technique has been popular in wired systems due to its low computational complexity, but the increase in the transmit signal power and associated degradation in bandwidth efficiency, although only a few percent, have so far deemed it undesirable in wireless systems [7]. In the case of the SLM technique, it was shown that while this technique can achieve excellent PAPR reduction, it has a high signal processing complexity due to the use of multiple inverse fast Fourier transform (IFFT) operations per OFDM block [8], [9]. Similar to the SLM technique, the PTS technique [10] requires several IFFT operations per OFDM symbol and while it can produce superior PAPR performance to the SLM technique it also has a higher complexity requirement and may require more side information (SI) bits. Both the SLM and PTS techniques have been of intense interest to many researchers who have proposed modifications with the aim to reduce the complexity and improve the performance of these techniques [10]–[14].

To optimize both complexity and PAPR reduction ability, we provide a novel PAPR reduction technique that operates on multiple time-domain OFDM symbols. Similar to the PTS technique, the principal idea of the proposed time-domain symbol combining (TDSC) technique is to create several different time-domain representations for each OFDM symbol and transmit the one(s) with the lowest PAPR. However, unlike the PTS technique in which the OFDM symbol is partitioned into several subsets and then each subset is individually IFFT-processed before performing the combinations in the time domain to form multiple time-domain representations, the TDSC technique creates various representations by intelligently forming linear combinations among consecutive time-domain OFDM symbols. Thus, the TDSC technique does not require more than one IFFT process per OFDM symbol while the PTS technique requires U IFFT operations per OFDM symbol, where U is the number of subsets used per OFDM block.

II. System Description

In this section, a brief description of the OFDM scheme as well as a definition of the PAPR problem are presented. At the OFDM transmitter, the information bit stream is first mapped to the symbols according to a certain modulation constellation,

Manuscript received May 3, 2007; revised May 22, 2008. First published July 9, 2008; current version published September 17, 2008. The associate editor coordinating the review of this paper and approving it for publication was Dr. Erchin Serpedin.

The authors are with the School of Electrical and Electronic Engineering, University of Manchester, Manchester, M60 1QD, U.K. (e-mail: e.alsusa@manchester.ac.uk; L.yang@ieee.org).

Color versions of one or more of the figures in this paper are available online at http://ieeexplore.ieee.org.

Digital Object Identifier 10.1109/TSP.2008.928161

such as M-ary phase-shift keying (M-PSK) or M-ary quadrature amplitude modulation (M-QAM), to create a vector of N complex-valued symbols, $X = [X_0, X_1, \ldots, X_{N-1}]$. Each complex symbol then modulates one orthogonal subcarrier and an OFDM signal is formed by summing all the N-modulated independent subcarriers that are of equal bandwidth and have a fixed frequency separation of $\Delta f = 1/NT$, where NT denotes the useful data block period. The mathematical representation of an OFDM time-domain signal, assuming a rectangular time-domain window [6], is given as

$$x(t) = \frac{1}{\sqrt{N}} \sum_{n=0}^{N-1} X_n \cdot e^{j2\pi n \Delta f t}, \qquad 0 \le t < NT \quad (1)$$

where $n = 0, 1, \ldots, N-1$. In the rest of this paper, a discrete-time representation of the OFDM signal will be used, which is expressed as

$$x_k = \frac{1}{\sqrt{N}} \sum_{n=0}^{N-1} X_n \cdot e^{j2\pi k n / LN}, \qquad k = 0, 1, \ldots, LN-1 \quad (2)$$

where L is the oversampling factor [15]. Therefore, the corresponding PAPR computed using the L times oversampled time-domain signal samples is given by

$$\frac{\max |x_k|^2}{E[|x_k|^2]} \quad (3)$$

where $E[|x|]$ is the average power of the $(N \cdot L)$ samples long time-domain OFDM symbol x.

III. PAPR Reduction

In this paper, we will compare the PAPR and complexity performance of the TDSC technique with the well-known SLM, PTS, and TR techniques due to the similarities shared between these three techniques and the TDSC. For example, the TDSC technique is similar in principle to the SLM and PTS techniques in the sense that it produces multiple time-domain signal representations per OFDM symbol, and also similar to the TR technique in the sense that both are time-domain-based techniques. Therefore, for the sake of completeness, a brief description of the SLM, PTS, and TR techniques will be provided first, followed by a description of the TDSC technique.

A. The SLM, PTS, and TR Techniques

The SLM technique belongs to the family of MSR PAPR reduction techniques and is based on a probabilistic approach for reducing the PAPR. Fig. 1 shows the system diagram of the ordinary SLM technique that uses U-independent vectors B each containing N random phase symbols. Each of the randomizing vectors is used to modify the phases of the vector of N complex baseband information symbols, which make up the frequency-domain OFDM symbol, in order to randomize their phases around the unit circle with the aim to produce a time-domain representation, after the IFFT operation, with a lower PAPR. Therefore, this process produces U new sets of phase-modified symbol vectors, $X \cdot B(1), X \cdot B(2), \ldots, X \cdot B(U)$ for each vector of N data symbols. After passing each of the U phase-modified vectors through the IFFT process, the vector with the best PAPR performance (i.e., a low-PAPR representative of the original symbol vector) will then be selected for transmission.

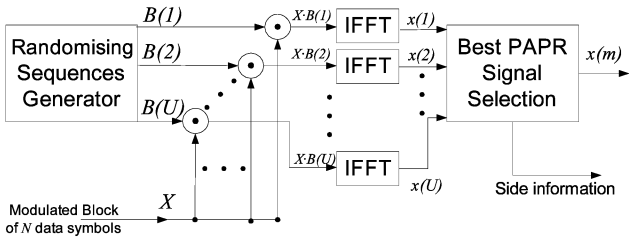

Fig. 1. Transmitter structure with the SLM technique.

In the case of the PTS technique, which also belongs to the same family of MSR techniques as the SLM technique, instead of randomizing the individual data symbols, each N-symbol vector is partitioned into U subsets, which are zero-padded to length N and then individually IFFT processed as shown in Fig. 2. By combining these subsets at the output of the IFFT processes using different bipolar or complex-number vectors, various representations for the original vector can be generated, from which the representation with the smallest PAPR is selected for transmission. It may already have become clear that this technique shares the same disadvantage of having to compute U IFFT operations per data vector, which significantly increases the system's complexity and hence the power consumption and time latency at the transmitter. In addition to the IFFT operations, there is also the combining process of the subsets in the time domain, which makes the PTS technique even more complex than SLM.

As for the TR technique, a subset of subcarriers is reserved at the transmitter for utilization in minimizing the PAPR of each OFDM symbol. That is, the subcarriers are divided into two disjoint frequency subspaces, one for the data X and one for PAPR reduction tones C, where $X_n = 0$, $n \in \{i_1, i_2, \ldots, i_V\}$, and $C_n = 0$, $n \notin \{i_1, i_2, \ldots, i_V\}$,, as shown in Fig. 3. Because the subcarriers are orthogonal, the V peak reduction carriers (PRCs) cause no distortion on the data bearing subcarriers and can simply be ignored at the receiver. In order for this technique to achieve a good PAPR reduction, it is vital that the PRCs are modulated with a suitable set of symbols. Therefore, the objective is to find the time-domain signal $c = \mathrm{IDFT}(C)$ to be added to the original time-domain signal x, such that the PAPR of the transmitted signal $x' = x + c = \mathrm{IDFT}(X + C)$ meets the required target. The values of the PRCs modulating symbols are estimated by solving a convex optimization problem. To solve such a problem, several methods with various degrees of complexity and performance were proposed in the literature, e.g., [7], [15], and [16].

While this technique provides excellent performance and has found applications in wired systems, its main disadvantage is the resulting reduction in bandwidth efficiency in the form of the redundant PRCs. Although such bandwidth reduction is not critical in wired systems, because there are typically unused subcarriers with signal-to-noise ratios (SNRs) too low for sending any information, and therefore, could be used for the PRCs, it was found that the best performance of this technique can only

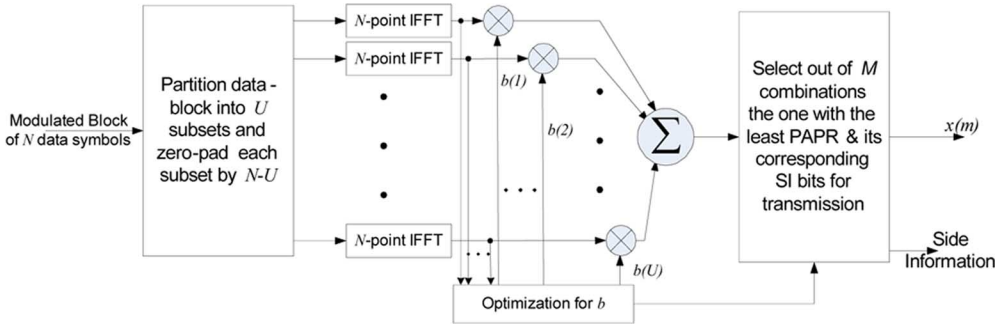

Fig. 2. Transmitter structure with the PTS technique.

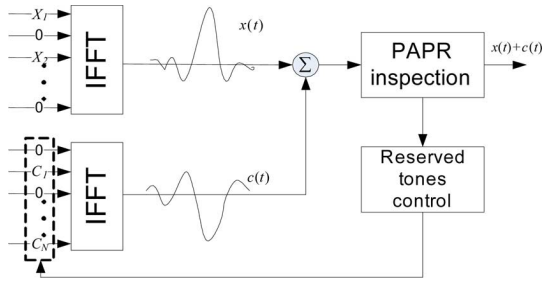

Fig. 3. Transmitter structure with the TR technique.

be achieved if the PRCs subcarriers are randomly selected per OFDM symbol and that if these subcarriers are selected to be in a continuous-block or nonuniform manner per OFDM block, the PAPR reduction capability of this technique will diminish [7]. In addition, in wireless systems, there is typically no fast reliable channel state feedback to dictate whether some subcarriers could be sacrificed for the PRCs, and therefore, a set of subcarriers must be reserved regardless of received SNRs, resulting in a costly bandwidth sacrifice.

B. The TDSC Technique

Similar to the SLM and PTS techniques, the TDSC technique [17] is also based on a probabilistic approach, and therefore, generates different representations for each OFDM symbol and transmits the one with the least PAPR. Unlike the PTS and SLM techniques, however, the TDSC technique only requires one IFFT operation per OFDM block. To generate different representations for each OFDM symbol, the TDSC technique exploits the variations between different time-domain OFDM symbols. This is achieved by linearly combining two or more different time-domain symbols together using various mathematical operations, which include addition, subtraction, and complex-conjugate operations. The combining process can be summarized using

$$d(k) = p_k \cdot \sum_{i=1}^{D} a \cdot m(i) \tag{4}$$

where $d(k)$ is the kth new combination, $k = 1, \ldots, F$, p_k is the power normalizing factor, D is the total number of symbols in the group, $a \in [-1 \quad 0 \quad 1]$, $m(i) \in \{x(i), x(i)^*\}$, $x(i)$, and $x(i)^*$ are the ith time-domain OFDM symbol and its complex conjugate, and F is the total number of combinations. Throughout the rest of this paper, the index in parentheses implies an array index as opposed to a sample index, which is signified by a lower index (subscript), and the combination is performed on a point-by-point basis. Additionally, data symbols represented by small letters indicate time domain while those represented by capital letters indicate frequency domain.

The basic operational mode of the TDSC technique is to combine two or more adjacent time-domain OFDM symbols for generating the various linear combinations. This mode of operation will be termed the adjacent symbol combining (ASC) mode in the rest of this paper. A special mode of operation of the TDSC technique is concerned with splitting the incoming time-domain symbols into groups of an even number of symbols, greater than two symbols per group, and dynamically combining these symbols in pairs. This approach is termed the dynamic symbol pairing (DSP) approach as no combination is made using more than two symbols. The difference between these two modes is that the ASC combines two or more *adjacent* symbols together while the DSP combines *only two* symbols together that may be adjacent or nonadjacent but must belong to the same group of symbols. Each of these modes produces different PAPR performance and is associated with different levels of complexity, memory usage, and latency. Both approaches will be described in detail below.

1) The ASC Mode: The ASC mode works on a group of adjacent time-domain OFDM symbols and their complex conjugates. To clarify the operation of this approach, let us suppose that the group consists of two time-domain OFDM symbols $x(1)$ and $x(2)$, i.e., $D = 2$. Considering the symbols and their complex conjugates, one can define two parent sets of symbols $P(1)$ and $P(2)$. Each parent set has four members (symbols or combination of symbols) as shown in Table I. Any two members, the ones which have the lowest PAPR, and are separable at the receiver, can be selected for transmission. It is noteworthy to mention that the parent sets consisting of $[x(1)^* \quad x(2)^*]$ and $[x(1)^* \quad x(2)]$ are not taken into consideration because their members would have the same PAPR as those in $P(1) = [x(1) \quad x(2)]$ and $P(2) = [x(1) \quad x(2)^*]$, respectively. Similarly, not all possible members need to be included in the parent sets when they have the same PAPR as other members already present in the parent set. For example, the members $\sqrt{1/2}(-x(1) - x(2))$ and $\sqrt{1/2}(-x(1) + x(2))$ do not need to be included in the parent set $P(1)$ as they

TABLE I
PARENT SETS AND CORRESPONDING MEMBER COMBINATIONS WITH $D = 2$

$P(1) = [x(1)\ x(2)]$	$P(2) = [x(1)\ x(2)^*]$
$x(1)$	$x(1)$
$x(2)$	$x(2)^*$
$\sqrt{1/2}(x(1) + x(2))$	$\sqrt{1/2}(x(1) + x(2)^*)$
$\sqrt{1/2}(x(1) - x(2))$	$\sqrt{1/2}(x(1) - x(2)^*)$

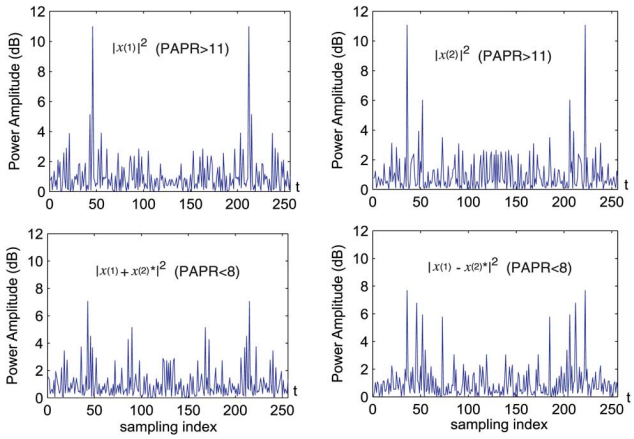

Fig. 4. Normalized power distribution of two time-domain OFDM symbols and two of their possible combinations, $N = 256$ subcarriers, $L = 1$.

have the same PAPR values as $\sqrt{1/2}(x(1) + x(2))$ and $\sqrt{1/2}(x(1) - x(2))$, respectively.

For illustration purposes, consider Fig. 4 ($D = 2$), which shows the PAPR for the members of $P(2)$. It is clear from this figure that the PAPR value can be reduced from 11 dB to around 7 dB by selecting the two members with the lowest PAPR. Note that this result is only valid for this particular example, which is just provided to give an insight into the operation of the ASC mode. Accurate results on the PAPR performance of this technique are presented in terms of the complementary cumulative distribution function (CCDF) in the results section.

The selection of the best members for transmission must be subject to the condition that these members are resolvable at the receiver. Therefore, even if the members $x(1) + x(2)$ and $x(1) + x(2)^*$ have the lowest PAPRs, they may not be selected for transmission if $x(1)$ and $x(2)$ cannot be deduced from the selected members at the receiver and hence a different pair, which may have a higher PAPR collectively, must be selected. The criterion used for ensuring that the selected members are resolvable will be discussed later in this paper.

By analogy, the same procedure can be extended for the case when there are more than two OFDM symbols per parent set (i.e., $D > 2$). The generalized number of parent sets Q and number of members per group R are given as

$$\begin{aligned} Q &= 2^{D-1} \\ R &= 2^{D-1} + D. \end{aligned} \tag{5}$$

For instance, $D = 3$ indicates a total of $2^{3-1} = 4$ parent sets and each of them has $2^2 + 3 = 7$ members in its group.

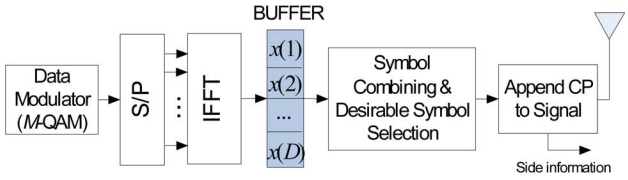

Fig. 5. Transmitter block diagram with the ASC technique.

The number of possible combinations from each parent set, assuming all combinations of members are resolvable at the receiver, is a binomial number $\binom{R}{D}$, which in this case gives $\binom{7}{3} = 35$, and the corresponding total number of possible combinations from all parent sets is 35. $Q = 140$. It will be shown later, however, that not all combinations of members will enable us to reproduce the symbols at the receiver, and hence, the total number of possible combinations that can be used is usually less than $\binom{R}{D} \cdot Q$. Due to the combination process, the resulting members will have a range of different PAPR values with the likelihood of including some members with lower PAPR than the original symbols. In this particular case, because the group consist of three time-domain symbols, three combinations must be selected for transmission.

It can be seen that as D is increased to 4 or more, the number of possibilities increases exponentially making it more likely to find members with very low PAPR. The penalties associated with increasing D, however, include the complexity of the selection from a large number of possibilities, some latency, increased number of side information bits as well as some BER performance degradation as will be discussed later in this paper.

Transmitter Structure: Fig. 5 shows a block diagram for the ASC-based OFDM system. The members of each parent set can be viewed as simultaneous equations that can be resolved at the receiver using the substitution or elimination methods. However, a more common technique is to use a matrix representation for the combining process. In this case, the combinations can be produced using a matrix multiplication between each parent set and a set of combining matrices. Such a way of producing the linear combinations can make it easier to both encode the side information bits associated with the combinations, which are necessary at the receiver to recover the original symbols, and perform the reverse combining process at the receiver. For example, for the above case in which the members $x(1) + x(2)$ and $x(1)$ are selected, the generation of these members can be represented using

$$\left[\sqrt{\tfrac{1}{2}}(x(1) + x(2)) \quad x(1)\right] = [x(1) \quad x(2)] \cdot \mathbf{h}(1) \tag{6}$$

where the combining matrix $\mathbf{h}(1) = \begin{bmatrix} \sqrt{1/2} & 1 \\ \sqrt{1/2} & 0 \end{bmatrix}$.

Similarly, each possible set of combinations can be represented in the form of a matrix multiplication. Each matrix is associated with a unique combination that is represented by the side information bits. It is essential to ensure that only combinations which have an invertible combining matrix are considered in the search for the best PAPR signal representations to enable the receiver to reverse the combining process. It must be acknowledged that while these constraints may reduce the PAPR reduction ability of the proposed technique, it is a necessity for

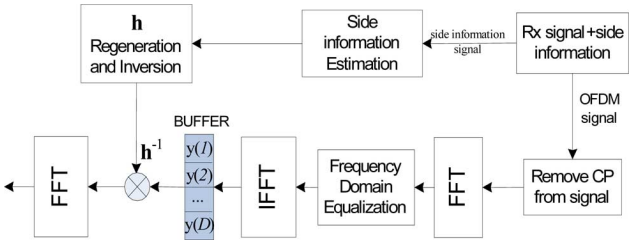

Fig. 6. Receiver block diagram with the ASC technique.

a proper operation of the TDSC technique. Through an exhaustive search which considered all the possible combinations for $D = 2, 3$, and 4, it was found that the total number of resolvable combinations is 12, 116, and 2560, respectively. That is, in the case of $D = 2$, all the possible combinations have invertible matrices, while in the case of $D = 3$ and $D = 4$, only 83% and 64%, respectively, of the total possible combinations have invertible matrices. It was also found that in all cases when the matrices are invertible, the smallest nonzero value the combing matrix's determinant can take is ± 0.707, ± 0.57, and ± 0.5 for $D = 2, 3$, and 5, respectively. The impact of this on the PAPR performance will be assessed in the results section.

If all possible invertible matrices are known at the receiver then reversing the combining process will be straightforward once the side information bits are correctly detected. The number of SI bits is determined by the number of invertible combining matrices used at the transmitter. For example, for the case of $D = 2$, because there are a total of 12 combinations from both parent sets, this means a minimum of $\log_2(12) \simeq 3.6$ bits of side information is required every two OFDM symbols.

Receiver Structure: A simplified block diagram for the receiver of the ASC approach is shown in Fig. 6. In the case when the selected members belong to parent-sets which contain complex-conjugated OFDM symbols it is necessary to perform the reverse-combining process in the time-domain, but after channel equalization which is usually implemented in the frequency domain. Therefore, after equalizing the received symbols, these symbols should be transformed back into time domain in order to recover the original OFDM symbols using the inverse of the same combining matrix applied at the transmitter as identified by the SI bits. The resolved signals are then transformed back to the frequency domain to complete the detection. Continuing with the previous example with $D = 2$ and the case of transmitting the members $x(1)$ and $\sqrt{1/2}(x(1) + x(2))$, assuming that the received symbols are equalized successfully, these symbols $[\,y(1) \quad y(2)\,]$ can be expressed as

$$[\,y(1) \quad y(2)\,] = [\,x(1) \quad x(2)\,] \cdot \mathbf{h}(1) + \Lambda \tag{7}$$

where Λ represents the additive channel noise. An estimate of the transmitted symbols $[\,\widetilde{x}(1) \quad \widetilde{x}(2)\,]$ can be obtained using

$$[\,\widetilde{x}(1) \quad \widetilde{x}(2)\,] = [\,y(1) \quad y(2)\,] \cdot \mathbf{h}(1)^{-1} \tag{8}$$

where $\mathbf{h}(1)^{-1} = \begin{bmatrix} 0 & \sqrt{2} \\ 1 & -1 \end{bmatrix}$.

While this method means that the receiver requires an extra I/FFT process, it can be possible to eliminate this requirement of extra FFT process if only parent sets that do not contain complex-conjugated time-domain symbols are considered, but this means that there will be fewer members to choose from at the transmitter. To describe how the reverse-combining process can be achieved in the frequency domain, we will continue with the same example as above where it is assumed that the members $\sqrt{1/2}(x(1) + x(2))$ and $x(1)$ were selected for transmission from the parent set $P(1) = [\,x(1) \quad x(2)\,]$, where $x(1)$ and $x(2)$ have $X(1)$ and $X(2)$ as their frequency-domain representations. Using the fact that $x(1) = X(1) \cdot W^{-1}$ and $x(2) = X(2) \cdot W^{-1}$, where W is an $N \times N$ matrix representing the Fourier transform, one can also see that $\sqrt{1/2}(x(1) + x(2)) = \sqrt{1/2}\left(X(1) \cdot W^{-1} + X(2) \cdot W^{-1}\right) = \sqrt{1/2}(X(1) + X(2)) \cdot W^{-1}$. Utilizing this relationship, it is easy to show that (see Appendix II) the received first and second symbols after the FFT operation are given as

$$Y(1) = \sqrt{\frac{1}{2}}(X(1) + X(2)) + \Upsilon(1)$$

and

$$Y(2) = X(1) + \Upsilon(2)$$

where $\Upsilon(1)$ and $\Upsilon(2)$ are vectors of additive white Gaussian noise (AWGN).

Therefore, it is possible to get both $X(1)$ and $X(2)$ without having to invoke an additional fast Fourier transform (FFT) operation using

$$[\,X(1) \quad X(2)\,] = [\,Y(1) \quad Y(2)\,] \cdot \mathbf{h}(1)^{-1}. \tag{9}$$

2) The DSP Mode: Although the DSP approach combines only two symbols together, the number of possible combinations is not limited to 12 as in the ASC approach when $D = 2$. This is because the DSP approach can consider all the possible pairings from a group of $K \geq 4$ symbols. The total number of possible pairings is given as

$$\prod_{i=0}^{(K/2)-1} (K - 2i - 1) \tag{10}$$

and because there are four members in each possible parent set, each pairing produces a total of $\binom{4}{2} = 12$ possibilities to choose from. That is, the total number of possible combinations is equal to $12 \cdot \prod_{i=0}^{(K/2)-1} (K - 2i - 1)$, from which K members, with the best PAPR, must be selected but with each two members belonging to the same parent set.

The biggest advantage of this approach is that it provides a large pool of possibilities, for instance, when $K = 4$ the total number of possible members is equal to $12 \cdot 3 = 36$, while the receiver has to operate on separating only two symbols at a time which results in less complexity at the receiver. The main disadvantage, however, is the larger number of symbols to be stored, which leads to longer latency. Nevertheless, this may not be in an issue for systems that employ time-domain interleavers to overcome the fading effects of the channel, and hence, have the memory to store a number of symbols.

The transmitter and receiver diagrams for the DSP approach are similar to the ASC with the exception that there is a slight difference in the process for generating the combinations at the transmitter and reversing that process at the receiver. Similar to the ASC approach, inverting the linear combinations at the receiver can be performed using matrix multiplication. However, in this case, it can either be done on every pair of arriving symbols or on the whole group of K symbols. For instance, assuming that the receiver is to reverse the combining process on the whole group of K symbols and that $K = 4$, given that the side information bits reveal the time indices of the members transmitted, i.e., $[\sqrt{1/2}(x(1)+x(2)) \quad x(2)]$ and $\sqrt{1/2}[x(3)-x(4) \quad x(3)+x(4)]$, then the received symbols $[y(1) \quad y(2) \quad y(3) \quad y(4)]$ can be expressed as $[y(1) \quad y(2) \quad y(3) \quad y(4)] = [x(1) \quad x(2) \quad x(3) \quad x(4)]\cdot\mathbf{h}(m) + \Lambda$, where in this case, it can be easily shown that

$$\mathbf{h}(m) = \begin{bmatrix} \sqrt{1/2} & 0 & 0 & 0 \\ \sqrt{1/2} & 1 & 0 & 0 \\ 0 & 0 & \sqrt{1/2} & \sqrt{1/2} \\ 0 & 0 & -\sqrt{1/2} & \sqrt{1/2} \end{bmatrix}.$$

Therefore, the estimated symbols

$$[\widetilde{x}(1) \quad \widetilde{x}(3) \quad \widetilde{x}(2) \quad \widetilde{x}(4)]$$

can be obtained using $[\widetilde{x}(1) \quad \widetilde{x}(3) \quad \widetilde{x}(2) \quad \widetilde{x}(4)] = [y(1) \quad y(2) \quad y(3) \quad y(4)] \cdot \mathbf{h}(m)^{-1}$, where in this case

$$\mathbf{h}(m)^{-1} = \begin{bmatrix} \sqrt{2} & 0 & 0 & 0 \\ -1 & 1 & 0 & 0 \\ 0 & 0 & \sqrt{1/2} & -\sqrt{1/2} \\ 0 & 0 & \sqrt{1/2} & \sqrt{1/2} \end{bmatrix}.$$

C. Complexity Comparison

It is well known that the minimum number of multiplications and additions required by the most common FFT technique which uses the Cooley–Tukey algorithm [19] can be expressed as

$$M_{\mathrm{IFFT}} = N \cdot \frac{\log_2 N}{2} \tag{11}$$

$$A_{\mathrm{IFFT}} = N \cdot \log_2 N. \tag{12}$$

Because SLM requires U IFFT processes, the number of multiplications M_{SLM} and additions A_{SLM} introduced by this technique are

$$M_{\mathrm{SLM}} = U \cdot N \cdot \left(\frac{\log_2 N}{2} + 1\right) \tag{13}$$

$$A_{\mathrm{SLM}} = U \cdot N \cdot \log_2 N. \tag{14}$$

Similarly, for the PTS technique, assuming U subsets, the number of multiplications M_{PTS} and additions A_{PTS} are given as

$$M_{\mathrm{PTS}} = N \cdot U \cdot \left(\frac{\log_2 N}{2}\right) \tag{15}$$

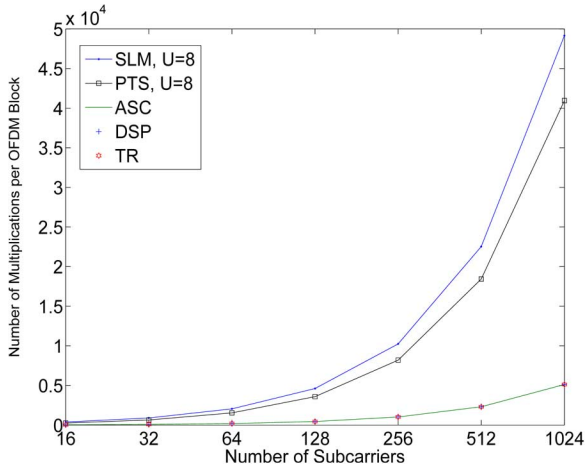

Fig. 7. Comparison of number of multiplications of SLM, PTS, TR, DSP, and ASC with different number of subcarriers.

$$A_{\mathrm{PTS}} = N \cdot \left(U \cdot \log_2 N + W^U - 1\right) \tag{16}$$

where W is the number of phase vectors of the combining vector used. Normally, four phases are considered to be sufficient for this in which case the value of $W = 4$.

In the case when the number of combinations of the PTS are constrained to the number of subsets, A_{PTS} is given as

$$A_{\mathrm{PTS}} = N \cdot (U \cdot \log_2 N + U - 1). \tag{17}$$

As for the time-domain techniques such as the TR and the proposed ASC and DSP approaches, their complexities depend mainly on the linear combination process which consists of a number of complex additions and subtractions, and therefore, the number of multiplications for the TR M_{TR}, ASC M_{ASC}, and DSP M_{DSP} techniques is only what is required by the IFFT process. That is

$$M_{\mathrm{DSP}} = M_{\mathrm{ASC}} = M_{\mathrm{TR}} = M_{\mathrm{IFFT}}. \tag{18}$$

As for the combined number of additions and subtractions per OFDM symbol, for the ASC A_{ASC}, DSP A_{DSP}, and TR A_{TR} techniques, these are found to be

$$\begin{aligned} A_{\mathrm{ASC}} &= N \cdot \left(\frac{2^{2(D-1)}}{D} + \log_2 N\right) \\ A_{\mathrm{DSP}} &= N \cdot (4 \cdot (K-1) + \log_2 N) \\ A_{\mathrm{TR}} &= N \cdot \log_2 N. \end{aligned} \tag{19}$$

The visual comparison for both the multiplication and addition/subtraction operations can be viewed from Figs. 7 and 8, respectively. As the TR, ASC, and DSP approaches require the same number of multiplications, only one technique is shown in Fig. 7. It can be seen from this figure that a significant complexity reduction is achieved with the ASC and DSP techniques, relative to the SLM and PTS techniques, especially as N is increased. In the case of the additions/subtraction comparison in Fig. 8, it is evident that, similar to the TR technique, the ASC and DSP can also provide substantial complexity savings with respect to the SLM and PTS techniques.

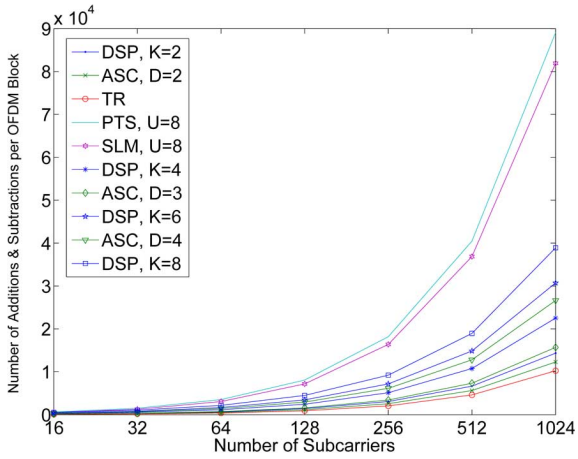

Fig. 8. Comparison of number of additions/subtractions of SLM, PTS, TR, DSP, and ASC techniques with different number of subcarriers.

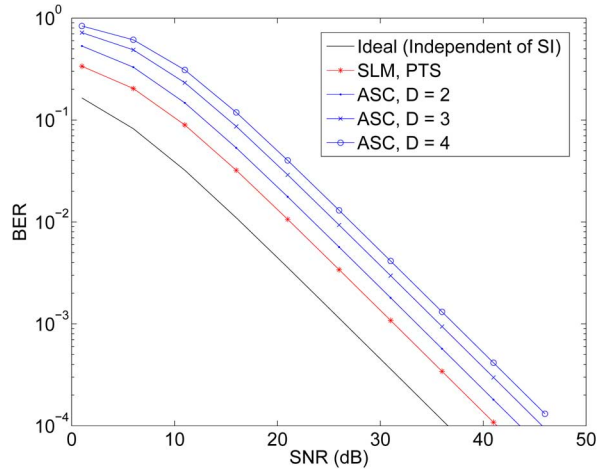

Fig. 9. BER performance assuming QPSK modulation for both the data and the side information bits, $N = 256$, $N_{SI} = 4, 6, 8$ for $D = 2, 3, 4$, respectively.

D. BER Comparison

It may already have become obvious that the combination of two or more symbols together implies that the success of separating these symbols relies on correct estimation of the associated side information bits. Similarly, in the case for PTS and SLM, correct detection of the side information is necessary to reverse the randomization processes. However, in the case of TDSC techniques, an additional concern is that an erroneous detection of the side information bits will result in incorrect estimation of all the symbols involved in the group, and hence, the possibility of higher system error rate due to error propagation between the different symbols combined. In this section, we will investigate the impact of the side information and symbols dependency on the BER performance of the system.

Assuming that the channel bit error rate (BER) is given as p_e, then the side information block error rate p_b is

$$p_b = 1 - (1 - p_e)^{N_{SI}}. \tag{20}$$

Given that the data BER probability independent of the side information is p, then the bit success probability of the data taking into account the dependence on the side information p_S can be approximated as

$$p_S = \begin{cases} \left(\frac{1}{2}\right)^D, & \text{incorrect SI} \\ (1-p), & \text{correct SI} \end{cases} \tag{21}$$

where D is the number of time-domain OFDM blocks included in the combination process. The upper half of this equation implies that the bit success rate in the case of the incorrect detection of the SI bits takes into account the dependence of D packets on the SI bits. In the case when the side information is correct, which is the lower half of the equation, the bit success rate is only a function of the BER. Expanding (21) produces

$$p_S = \left(\frac{1}{2}\right)^D \cdot p_u + p_l \tag{22}$$

where $p_u = \left(1 - (1 - p_e)^{N_{\mathrm{SI}}}\right)$, and $p_l = (1-p)\cdot(1 - p_e)^{N_{\mathrm{SI}}}$.

Because we are interested in the BER including the dependency on the SI bits p_B, this is given as

$$\begin{aligned} p_B &= 1 - p_S \\ &= 1 - \left[\left(\frac{1}{2}\right)^D \cdot p_u + p_l\right]. \end{aligned} \tag{23}$$

If both the data and side information bits go through the same channel, and therefore, have the same BER, i.e., $p = p_e$, then p_B can be written as

$$p_B = 1 - \left[\left(\frac{1}{2}\right)^D \cdot p_u + (1 - p_e)^{(N_{SI}+1)}\right]. \tag{24}$$

The above same equation, with D replaced by 1, also applies to the case of the SLM and PTS techniques. It is clear from this that when the SLM and PTS techniques require the same number of side information bits the BER performance for those two techniques will be identical.

Assuming M-PSK modulation, because each subcarrier is subjected to flat-fading, the BER can be given as [18]

$$p_e = \lambda \cdot \left[1 - \sqrt{\frac{g_m\gamma}{1 + g_m\gamma}} \cdot \left(\frac{M}{(M-1)\times\pi}\right) \cdot p_g\right] \tag{25}$$

where

$$p_g = \left[(\pi/2) + \tan^{-1}\left(\sqrt{(g_m\gamma/1+_{g_m\gamma})} \cdot \cot(\pi/M)\right)\right]$$

$\lambda = (1/\log 2(M)) \cdot (M - 1/M)$, $g_m \triangleq \sin^2(\pi/M)$, M is the number of symbols in the constellation, and γ is the average SNR per symbol.

While modified implementations of the SLM technique in which the side information can be avoided, e.g., [21], at the expense of some additional receiver complexity, in the comparison presented here, we only consider the conventional SLM implementation that requires side information. In Fig. 9, (24) is plotted to examine and compare the effect of side information bits on both the SLM and ASC techniques. In this case,

although the PTS technique normally requires more side information than the SLM technique, for simplicity, we will assume that the PTS technique requires the same number of side information bits, and therefore, its BER performance is identical to that of the SLM. It is noteworthy to mention here that the BER performance in the case of the DSP approach is identical to that of the ASC approach when $D = 2$. In this comparison, both the data and the side information are assumed to be QPSK-modulated and are carried by subcarriers which are subjected to independent flat-fading channels. It can be seen from this figure that when compared with the ideal case, in which the side information is always correctly detected, both techniques suffer a loss in performance due to the reliance of the data bits on correct detection of the side information bits. Although the TR technique has a BER performance that is independent of any side information, the penalty for this is the associated bandwidth reduction entailed due to the redundant PRCs. The SLM technique is slightly superior to the ASC technique as more than one block of data is dependent on the SI bits in the case of ASC technique. In this particular example, the number of SI bits was chosen to be 4, 6, and 8 for $D = 2, 3$, and 4, and for the SLM with $U = 8$ the number of SI bits used was 3. Obviously, as D increases, more SI bits are required and hence the BER performance of the ASC degrades. To minimize the BER performance degradation of both the SLM and ASC techniques, an appropriate investment of more power in the SI bits can prove useful. It can be seen from Fig. 10 that the difference in performance between the SLM and the ASC technique improves radically as more power is invested in the side information bits, which makes their detection much more reliable at the receiver. The results shown are the BER versus the ratio of the average power invested per SI and per data bit (SDPR). In (23), if p_e is virtually zero, i.e., correct detection of the SI bits, $p_B = p_b$. This would be correct if the power investment in the SI bits was not subtracted from the data bits. Normally, however, the extra investment of power in the SI bits comes at the expense of less power investment in the data bits, which is the reason why the performances of the ASC and SLM techniques never reach the performance of the ideal case in which perfect detection of the SI bits is assumed when SDPR $= 0$ dB. It can also be seen from this figure that excessive investment of the power in the SI bits (i.e., when SDPR $\gg 15$ dB) can lead to worse performance as power invested in the SI bits is power withdrawn from the data bits. It is important to highlight here that at $D = 2$, the ASC technique and hence the DSP technique have the same BER performance as the SLM technique when SDPR $= 10$ dB. When D increases beyond 2, the difference in performance between the SLM and ASC techniques increases, but only marginally and remains negligible when the optimal SDPR value is chosen. Usually, in practice, however, instead of increasing the power in the SI bits, strong forward error correction coding is applied on the SI bits to ensure that BER performance of these bits is radically diminished. Similarly, the information symbols would also be FEC encoded in most practical systems so that much better BER performances can be achieved and at lower SNR values.

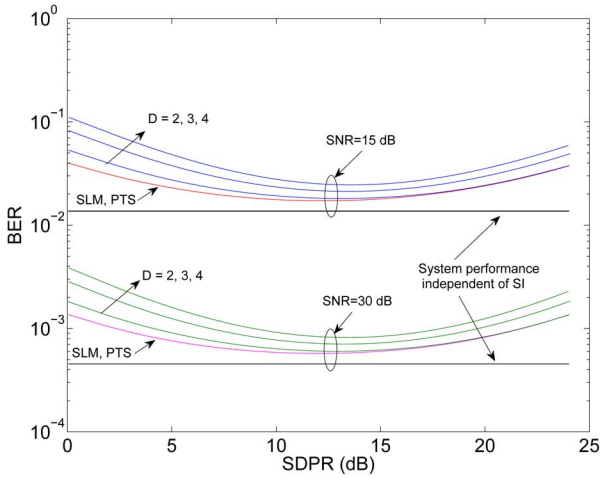

Fig. 10. BER performance assuming QPSK modulation for both the data and the side information bits over various side information to data symbols power ratio (SDPR), $N = 256$, $N_{SI} = 4, 6, 8$ for $D = 2, 3, 4$, respectively.

IV. Numerical Results

In this section, we will report on several simulation results to evaluate the PAPR performance of the proposed TDSC technique. The complementary cumulative density function of the PAPR is used to measure the performance. The CCDF of the PAPR is defined as

$$\mathrm{CCDF}(\mathrm{PAPR}(x(k))) = \Pr(\mathrm{PAPR}(x(k)) > \zeta) \qquad (26)$$

where ζ is a certain threshold value that is usually given in decibels relative to the root mean square (RMS) value.

The simulations below are performed for the OFDM system with a 256-point and 1024-point Fourier transform under the condition of an oversampling factor $L = 4$. Both QPSK and 16-QAM modulation techniques are examined here. The results shown below are based on the averaging of 100 000 OFDM per measured PAPR point. For all the ASC and DSP results shown in this section, except for Fig. 15, only the member combinations that have invertible matrices are used. That is, for $D = 2, 3$, and 4, the number of combinations used were 12, 116, and 2560, respectively.

The CCDFs of the PAPR for 256 subcarriers with QPSK modulation and different number of combinations are shown in Fig. 11. These results also include performances of the SLM and PTS techniques with eight randomizing sequences and the TR technique with 5% PRCs. It is clear that for less than 0.001% of the data blocks, the unmodified OFDM signal has a PAPR over 12 dB and the SLM, PTS, and TR techniques can reduce it to 8.9, 9, and 8.7 dB, respectively. On the other hand, the 0.001% PAPR of the proposed ASC technique is 8.7, 9.3, and 10.2 dB, for $D = 4$, $D = 3$, and $D = 2$, respectively. Although the performance with $D = 3$ is close to the SLM and PTS techniques, it is clear that the performance gets better when D is increased to 4. It can be seen that the proposed ASC can provide excellent PAPR reduction performance and with significantly less complexity than both the SLM and PTS techniques. This comparison was repeated for the case of 16-QAM and $N = 1024$ and

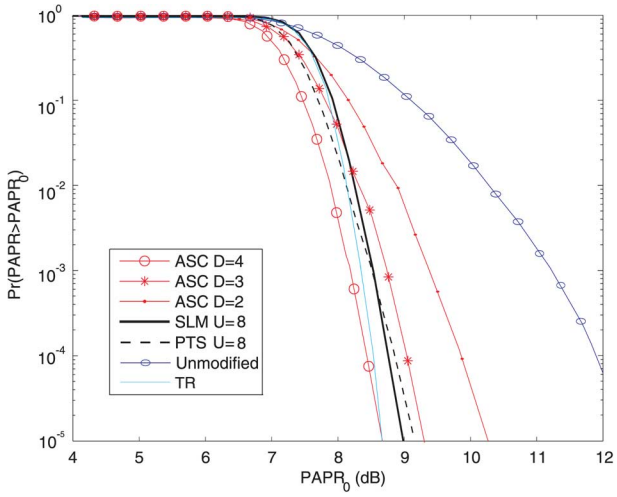

Fig. 11. CCDF of ASC-modified OFDM signals with different buffer sizes using QPSK with $N = 256$.

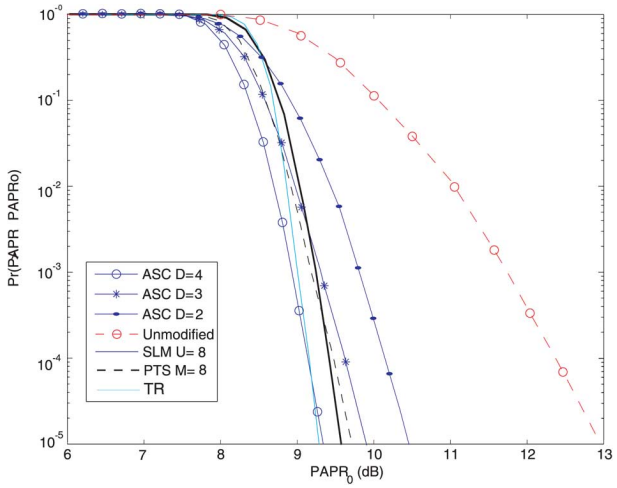

Fig. 12. CCDF of ASC-modified OFDM signals with different buffer sizes using 16-QAM with $N = 1024$.

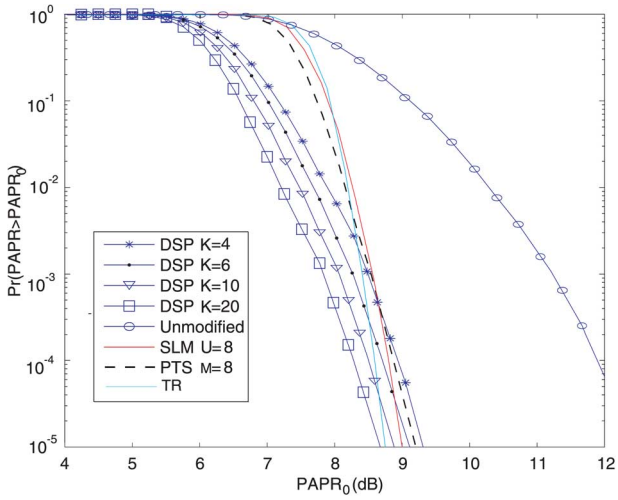

Fig. 13. CCDF of DSP-modified OFDM signals with different buffer sizes with QPSK and $N = 256$.

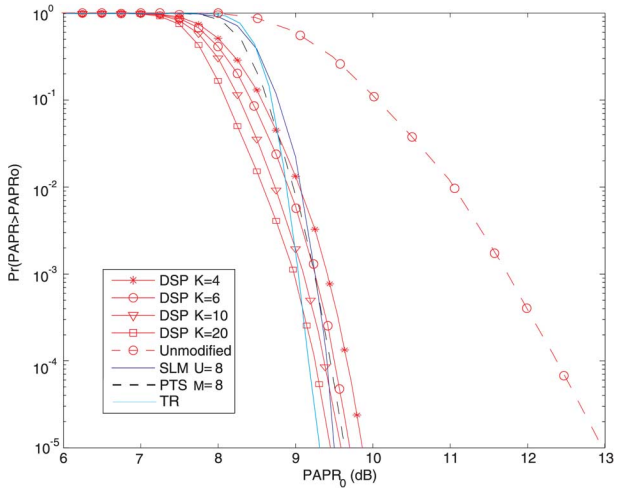

Fig. 14. CCDF of DSP-modified OFDM signals with different buffer sizes with 16-QAM and $N = 1024$.

the results are shown in Fig. 12. It is evident from this figure that similar conclusions as before can be deduced.

For clarity, the results for the DSP mode are shown separately in Figs. 13 and 14, which are again showing the CCDF of the PAPR for 256 subcarriers with QPSK modulation and 1024 subcarriers with 16-QAM modulation, respectively. Similar to the results of the ASC mode, for comparison purposes, these figures also include performances of the SLM, the PTS with $U = 8$ for both techniques, and the TR technique with 5% PRCs. It is clear that the DSP technique outperforms the reference techniques in 99.9% transmitted symbols; only less than 0.01% symbols have a performance loss within 0.5 dB.

By comparing the results in Figs. 11 and 13, it is obvious that both the ASC and DSP modes achieve similar PAPR performances as the SLM, PTS, and TR techniques for $D = 3$, $K = 4$, and $U = 8$. Both the ASC and DSP techniques have much lower complexity than the SLM and PTS for these parameters and cause less degradation in bandwidth efficiency than the TR technique. On the other hand, for both the ASC and DSP modes, the BER performance is slightly worse than that of the SLM and TR. This BER degradation, however, can be minimized significantly by ensuring that the SI bits are better protected by either investing more power in the SI bits, or using strong forward error correction coding for these bits. This will improve the SI bits detection reliability at the receiver, and consequently, improve the system's BER performance significantly.

In Fig. 15, we present results for the ASC technique to illustrate the impact of varying the number of used member combinations on the PAPR reduction ability of this technique. In this figure, 100% corresponds to all the possible combinations that include the combinations with noninvertible combining matrices. It is shown in this figure that the majority of the PAPR is achieved within the first 50% of the total number of combinations for both when $D = 3$ and $D = 4$. It is also evident from both curves that discarding the percentage of possibilities,

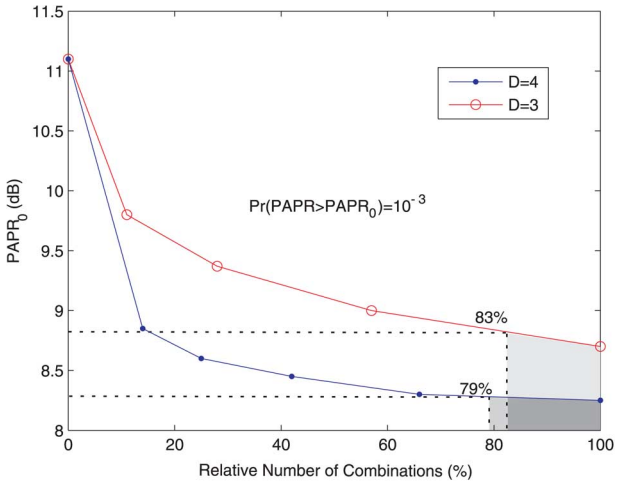

Fig. 15. PAPR performance as a function of varying the number of combinations used. The x-axis is in percentage relative to the maximum number of all possible combinations.

which have noninvertible matrices, causes a marginal degradation of the achievable PAPR.

V. Conclusion

The time-domain symbol combining PAPR reduction technique proposed in this paper was shown to provide excellent PAPR reductions and at lower complexities, especially in terms of the number of multiplications, when compared to the powerful SLM, PTS, and TR techniques. As in most if not all signal processing techniques, the proposed technique has some drawbacks. For example, similar to the conventional SLM and PTS techniques, the correct detection of the received data blocks is dependent on correctly estimating the side information bits necessary for reversing the randomization process. This drawback, however, can be overcome by protecting the side information bits further through the use of FEC coding such that the BER of these bits is extremely small. Also, similar to the SLM and PTS techniques, the TDSC technique requires processing at the receiver side. While the SLM and PTS techniques require to reverse the randomization process that takes place at the transmitter the TDSC technique may require an extra I/FFT process to reverse the combing process. Finally, unlike the SLM, PTS, and TR techniques, the TDSC technique entails some latency at the receiver due to requiring the availability of all symbols involved to reverse the combining process. Such latency, however, may not be a problem for communication systems, which use interleaving. The results provided by the complexity, BER, and PAPR figures can be used collectively as a guide to provide the best operational parameters for both the ASC and DSP modes of operation depending on the application under consideration.

Appendix I

To evaluate the probability that an OFDM symbol exhibits a peak whose absolute value $|x(n)|$ exceeds a certain threshold $|\bar{x}|$, or equivalently, the probability that the normalized power exceeds the value $(|\bar{x}|/\sigma_x) = \sqrt{\mathrm{PAPR}_0}$, one uses the cumulative distribution function (CDF) for the PAPR of an OFDM signal, which is defined as

$$\begin{aligned}\mathrm{CDF}(\mathrm{PAPR}_0) &= \Pr(\max|x(n)| < |\bar{x}|) \\ &= \Pr(\mathrm{PAPR}(x(n)) < \mathrm{PAPR}_0). \end{aligned} \quad (27)$$

Assuming that the absolute values of the time-domain OFDM signal samples are distributed according to the Rayleigh function

$$f(x) = \frac{2x}{\sigma_x^2} e^{-\left(x^2/\sigma_x^2\right)} \quad (28)$$

where $E(|\mathrm{Re}(x(n))|^2) = \sigma_x^2$. To evaluate which is the probability that an OFDM symbol exhibits a peak whose absolute value $|x_n|$ exceeds a certain value $|\bar{x}|$, or equivalently, the probability that the normalized power exceeds the value $(|\bar{x}|/\sigma_x) = \sqrt{\mathrm{PAPR}_0}$, the CDF for the PAR of an OFDM signal is defined as

$$\begin{aligned}\mathrm{CDF}\left(\mathrm{PAPR}_0\right) &= \Pr(\max|x(n)| < |\bar{x}|) \\ &= \Pr\left(\mathrm{PAPR}(x(n)) < \mathrm{PAPR}_0\right). \end{aligned} \quad (29)$$

Integrating 28, we obtain

$$\begin{aligned}\Pr\left(|x(n)| < |\bar{x}|\right) &= 1 - \int_{|\bar{x}|}^{\infty} f(x)dx \\ &= 1 - e^{-\mathrm{PAPR}_0}. \end{aligned} \quad (30)$$

Due to the independence of the N samples, the CDF of the PAPR of a data block with Nyquist rate sampling is derived as

$$\Pr\left(\mathrm{PAPR}(x(n)) < \mathrm{PAPR}_0\right) = \left(1 - e^{-\mathrm{PAPR}_0}\right)^N \quad (31)$$

and the CCDF can be expressed

$$\begin{aligned}P &= \Pr\left(\mathrm{PAPR}(x(n)) > \mathrm{PAPR}_0\right) \\ &= 1 - \left(1 - e^{-\mathrm{PAPR}_0}\right)^N. \end{aligned} \quad (32)$$

Because the selection process of ASC can be regarded as a binomial distribution within each parent group, the probability of at least D symbols having PAPR values larger than the threshold PAPR_0, $\Pr(A)$, can be expressed as

$$\begin{aligned}\Pr(A) &= 1 - \sum_{k=0}^{D-1} \Pr\left(B_k\right) \\ &= 1 - \sum_{k=0}^{D-1} \binom{R}{k} P^k (1-P)^{R-k} \end{aligned} \quad (33)$$

where B_k is the event when there are k symbols with values larger than $PAPR_0$. Therefore, the CDF within each parent group $\Pr(C)$ is

$$\Pr(C) = \sum_{k=0}^{D-1} \binom{R}{k} P^k (1-P)^{R-k}. \quad (34)$$

TABLE II
CCDF OF ANALYTICAL AND SIMULATION RESULTS FOR ASC WITH $D = 3$, AND UNMODIFIED OFDM SYMBOLS, USING $N = 256$

CCDF(dB) ($\text{PAPR}>\text{PAPR}_0$)	Unmodified Simulation	Unmodified Analytical	ASC Simulation	ASC Analytical
Pr(PAPR>7)	0.9	0.82	0.8	0.98
Pr(PAPR>7.5)	0.6	0.60	0.2	0.67
Pr(PAPR>8)	0.4	0.37	0.06	0.07
Pr(PAPR>8.5)	0.2	0.19	0.002	0.0004

Because the total number of parent groups is 2^{D-1}, the probability of having at least one group with $\text{PAPR} < \text{PAPR}_0$ can be obtained by using binomial distribution again as

$$\begin{aligned}&\text{CDF}_{\text{ASC}}\left(\text{PAPR}_0\right)\\ &\quad= 1 - \underbrace{\binom{2^{D-1}}{0}\Pr\left(C\right)^0\left(1-\Pr\left(C\right)\right)^{2^{D-1}-0}}_{\text{No group with PAPR}<\text{PAPR}_0}\\ &\quad= 1 - \left(1 - \sum_{k=0}^{D-1}\binom{R}{k}P^k(1-P)^{R-k}\right)^{2^{D-1}}. \quad (35)\end{aligned}$$

A comparison between results obtained by the above expressions and the simulation results are presented in Table II. The analytical results are shown to be reasonably close to the simulation results, especially in the unmodified case. It is also evident from this table that the analytical results for the ASC technique deviate from the simulation results as PAPR_0 increases beyond 8 dB. The reason for this could be due to the relaxed assumption that all the signal representation members are independent when in fact some of these members, especially the combinational ones, may not be independent.

APPENDIX II

The received first symbol $z(1)$ is equivalent to the transmitted symbol convolved with the channel impulse response and corrupted by AWGN. That is

$$z(1) = \left(\sqrt{\frac{1}{2}}\left(X(1)+X(2)\right)\cdot W^{-1}\right) * \hbar(1) + \eta(1) \quad (36)$$

where the symbol $*$ implies convolution, $\hbar(1)$ is the channel impulse response, and $\eta(1)$ is AWGN. After the FFT process is invoked, the frequency-domain first symbol $Z(1)$ is given as

$$Z(1) = \left(\left(\sqrt{\frac{1}{2}}\left(X(1)+X(2)\right)\cdot W^{-1}\right) * \hbar(1) + \eta(1)\right)\cdot W. \quad (37)$$

Assuming that a cyclic prefix of equal length to the channel maximum delay spread is appended at the beginning of every transmitted symbol [1], (37) can be simplified to

$$Z(1) = \sqrt{\frac{1}{2}}\left(X(1)+X(2)\right)\cdot H(1) + V(1) \quad (38)$$

where $H(1) = \hbar(1)\cdot W$ is the channel frequency response and $V(1) = \eta(1)\cdot W$. Assuming that the receiver is able to estimate the channel frequency response, the equalized received signal is

$$\begin{aligned}Y(1) &= \frac{\sqrt{\frac{1}{2}}\left(X(1)+X(2)\right)\cdot H(1) + V(1)}{H(1)}\\ &= \sqrt{\frac{1}{2}}\left(X(1)+X(2)\right) + \Upsilon(1) \quad (39)\end{aligned}$$

where $\Upsilon(1) = V(1)/H(1)$ and the division operation is performed on a point-by-point basis.

Similarly, for the second received symbol, we get

$$\begin{aligned}Z(2) &= \left(\left(X(1)\cdot W^{-1}\right) * \hbar(2) + \eta(2)\right)\cdot W\\ &= X(1)\cdot H(2) + V(2) \quad (40)\end{aligned}$$

and

$$\begin{aligned}Y(2) &= \frac{X(1)\cdot H(2) + V(2)}{H(2)}\\ &= X(1) + \Upsilon(2). \quad (41)\end{aligned}$$

REFERENCES

[1] L. Cimini, Jr, "Analysis and simulation of a mobile radio channel using orthogonal frequency division multiplexing," *IEEE Trans. Commun.*, vol. 33, no. 7, pp. 665–675, Jul. 1985.

[2] C. Eklund, R. B. Marks, K. L. Stanwood, and S. Wang, "IEEE standard 802.16: A technical overview of the wirelessMAN air interface for broadband wireless access," *IEEE Commun. Mag.*, vol. 40, no. 6, pp. 98–107, Jun. 2002.

[3] H. Sari, G. Karam, and I. Jeanclaude, "Transmission techniques for digital terrestrial tv broadcasting," *IEEE Commun. Mag.*, vol. 33, no. 2, pp. 100–109, Feb. 1995.

[4] B. Ai, Z. Yang, C. Pan, Zhang, T. Tao, and J. Ge, "Effects of PAPR reduction on HPA predistortion," *IEEE Trans. Consumer Electron.*, vol. 51, no. 4, pp. 1143–1147, Nov. 2005.

[5] H. Ochiai and H. Imai, "On the distribution of the peak-to-average power ratio in OFDM signals," *IEEE Trans. Commun.*, vol. 49, no. 2, pp. 282–289, Feb. 2001.

[6] S. H. Han and J. H. Lee, "An overview of peak-to-average power ratio reduction techniques for multicarrier transmission," *IEEE Wireless Commun.*, vol. 12, no. 2, pp. 56–65, Apr. 2005.

[7] J. Tellado, "Peak to average power reduction for multicarrier modulation," Ph.D. dissertation, Dept. Electr. Eng., Stanford Univ, Stanford, CA, 2000.

[8] S. H. Müller, R. W. Bäuml, R. F. H. Fischer, and J. B. Huber, "OFDM with reduced peak-to-average power ratio by multiple signal representation," *Ann. Telecommun.*, vol. 52, no. 1–2, pp. 58–67, Feb. 1997.

[9] R. W. Bäuml, R. F. H. Fischer, and J. B. Huber, "Reducing the peak-to-average power ratio of multicarrier modulation by selected mapping," *Electron. Lett.*, vol. 32, no. 22, pp. 2056–57, Oct. 1996.

[10] G. Lu, P. Wu, and C. Carlemalm-Logothetis, "Peak-to-average power ratio reduction in OFDM based on transformation of partial transmit sequences," *Electron. Lett*, vol. 42, pp. 105–106, 2006.

[11] Y. C. Cho, S. H. Han, and J. H. Lee, "Selected mapping technique with novel phase sequences for PAPR reduction of an OFDM signal," in *Proc. IEEE 60th Veh. Technol. Conf.*, Sep. 2004, vol. 7, pp. 4781–4785.
[12] G. Lu, P. Wu, and C. Carlemalm-Logothetis, "Enhanced interleaved partitioning PTS for peak-to-average power ratio reduction in OFDM systems," *Electron. Lett.*, vol. 42, pp. 983–984, 2006.
[13] H. H. Seung and H. L. Jae, "PAPR reduction of OFDM signals using a reduced complexity PTS technique," *IEEE Signal Process. Lett.*, vol. 11, no. 11, pp. 887–890, Nov. 2004.
[14] L. Dae-Woon, N. Jong-Seon, L. Chi-Woo, and C. Habong, "A new SLM OFDM scheme with low complexity for PAPR reduction," *IEEE Signal Process. Lett.*, vol. 12, no. 2, pp. 93–96, Feb. 2005.
[15] A. Gatherer, M. Polley, T. I. Inc, and T. X. Dallas, "Controlling clipping probability in DMT transmission," in *Proc. 31st Asilomar Conf. Signal Syst. Comput.*, Nov. 1997, vol. 1, pp. 578–584.
[16] B. S. Krongold and D. L. Jones, "A new tone reservation method for complex-baseband PAR reduction in OFDM systems," *Acoust. Speech Signal Process.*, vol. 3, pp. 2321–2324, 2002.
[17] C. Tellambura, "Computation of the continuous-time PAR of an OFDM signal with BPSK subcarriers," *IEEE Commun. Lett.*, vol. 5, no. 5, pp. 185–187, May 2001.
[18] E. Alsusa and L. Yang, "A new PAPR reduction technique using time domain symbol scrambling for OFDM systems," in *Proc. IEEE Int. Symp. Signal Process. Appl.*, Feb. 2007, pp. 873–877.
[19] C. I. Emmanuel and W. J. Barrie, *Digital Signal Processing: A Practical Approach*. Englewood Cliffs, NJ: Prentice-Hall, 1993.
[20] M. K. Simon and M. S. Alouini, *Digital Communications Over fading Channels*, 2nd ed. New York: Wiley-Interscience, 2004.
[21] E. Alsusa and L. Yang, "Redundancy-free and BER-maintained selective mapping with partial phase-randomizing sequences for PAPR reduction in OFDM systems," *IET Commun.*, vol. 2, no. 1, pp. 66–74, Jan. 2008.
[22] D. P. Bertsekas and J. N. Tsitsiklis, *Introduction to Probability*. Belmont, MA: Athena Scientific, 2002.

Emad Alsusa (M'06–SM'07) received the B.Sc. degree in electrical and electronic engineering from Salford University, Salford City, U.K., in 1996 and the Ph.D. degree in electrical and electronic engineering from Bath University, Bath, U.K., in 2000.

From June 2000 to September 2003, he was a Postdoctoral Research Fellow at the School of Engineering and Electronics, Edinburgh University, U.K. He joined Manchester University, Manchester, U.K., in 2003 as a Lecturer of Communication Engineering. His research interests are in the area of wireless communication networks, especially, modulation and multiple access techniques, channel estimation, coding, multiuser detection, and multiple-input–multiple-output (MIMO) techniques.

Lin Yang (S'04) received with B.Eng. degree in electrical engineering and electronics from the Bejing Institute of Technology, Beijing, China, in 2003 and the M.Sc. degree with distinction from University of Manchester Institute of Science and Technology, Manchester, U.K., in 2004. He is currently working towards the Ph.D. degree in electrical and electronic engineering at the University of Manchester.

His interests include OFDM systems, PAPR problem of multicarrier systems, and mobile communications.